

Oxidative Addition to U(V)–U(V) Dimers: Facile Routes to Uranium(VI) Bis(imido) Complexes

Liam P. Spencer,[†] Ping Yang,[‡] Brian L. Scott,[†] Enrique R. Batista,[‡] and James M. Boncella^{*†}

[†]Materials, Physics and Applications Division, Los Alamos National Laboratory, MS J514, Los Alamos, New Mexico 87545, and [‡]Theoretical Division, Los Alamos National Laboratory, MS B268, Los Alamos, New Mexico 87545

Received August 7, 2009

The ability of dimeric bis(imido) uranium(V) complexes with the general formula $[U(N^tBu)_2(Y)(^tBu_2bpy)]_2$ ($Y = I$ (**1**), SPh (**2**); $^tBu_2bpy = 4,4'$ -di-*tert*-butyl-2,2'-bipyridyl) to behave as two-electron reducing agents was examined with I_2 , AgX ($X = Cl, Br$), PhEPh ($E = S, Se, Te$), and chalcogen (O, S, Se) atom transfer reagents. The addition of I_2 and AgX to **1** leads to the formation of uranium(VI) dihalide complexes with the general formula $U(N^tBu)_2(I)(X)(^tBu_2bpy)$ ($X = I$ (**3**), Cl (**4**), Br (**5**)). Complexes **1** and **2** can also reduce PhEPh to generate uranium(VI) complexes with the general formula $U(N^tBu)_2(X)(EPh)(^tBu_2bpy)$ ($X = I, E = S$ (**6**), Se (**8**), Te (**10**); $X = SPh, E = S$ (**7**), Se (**12**)). These unsymmetrical complexes appear to be in equilibrium with the uranium(VI) complexes $U(N^tBu)_2(X)_2(^tBu_2bpy)$ and $U(N^tBu)_2(EPh)_2(^tBu_2bpy)$ ($E = Se$ (**9**), Te (**11**)) and suggest that both U–I and U–E bonds possess a labile nature in bis(imido) uranium(VI) complexes. Complex **1** also reacts as a two-electron reductant toward chalcogen atom transfer reagents such as 4-methylmorpholine N-oxide, S_8 , and Se to produce dimeric bis(imido) uranium(VI) complexes with the general formula $[U(N^tBu)_2(I)(^tBu_2bpy)]_2(\mu-E)$ ($E = O$ (**13**), S (**14**), Se (**15**)) and $[U(N^tBu)_2(I)(^tBu_2bpy)]_2(\mu-\eta^2:\eta^2-E_4)$ ($E = S$ (**16**), Se (**17**)). Density functional theory studies performed on a model complex of **13** indicate the presence of multiple bonding in the bridging U–O bond.

Introduction

Actinide materials have long held promise to accomplish catalysis and chemical transformations that are distinct from their transition metal counterparts. Though not as mature as transition metal chemistry, actinide elements hold promise in these areas due to their ability to form complexes with large formal coordination numbers, their unusual coordination geometries, and their ability to attain a variety of stable oxidation states.¹ Interest in this area has been focused on organouranium chemistry which, in addition to these attributes, has also shown an aptitude to promote multielectron transfer reactions to organic substrates. This phenomenon can be achieved by both metal- and ligand-based reductions

and involves the transfer of up to eight electrons, depending upon the uranium/ligand combination.^{2–5}

(3) (a) Brennan, J. G.; Andersen, R. A. *J. Am. Chem. Soc.* **1985**, *107*, 514–516. (b) Brennan, J. G.; Andersen, R. A.; Zalkin, A. *Inorg. Chem.* **1986**, *25*, 1756–1760. (c) Brennan, J. G.; Andersen, R. A.; Zalkin, A. *Inorg. Chem.* **1986**, *25*, 1761–1765. (d) Zalkin, A.; Brennan, J. G.; Andersen, R. A. *Acta Crystallogr.* **1988**, *C44*, 1553–1534. (e) Stults, S. D.; Andersen, R. A.; Zalkin, A. *Organometallics* **1990**, *9*, 1623–1629. (f) Bethet, J.-C.; Le Marechal, J.-F.; Nierlich, M.; Lance, M.; Vigner, J.; Ephritikhine, M. *J. Organomet. Chem.* **1991**, *408*, 335–341. (g) Avens, L. R.; Barnhart, D. M.; Burns, C. J. *Inorg. Chem.* **1994**, *33*, 4245–4254. (h) Roussel, P.; Boaretto, R.; Kingsley, A. J.; Alcock, N. W.; Scott, P. *J. Chem. Soc., Dalton Trans.* **2002**, 1423–1428. (i) Castro-Rodriguez, I.; Olsen, K.; Gantzel, P.; Meyer, K. *J. Am. Chem. Soc.* **2003**, *125*, 4565–4571. (j) Bart, S. C.; Anthon, C.; Heinemann, F. W.; Bill, E.; Edelstein, N. M.; Meyer, K. *J. Am. Chem. Soc.* **2008**, *130*, 12536–12546.

(4) (a) Graves, C. R.; Scott, B. L.; Morris, D. E.; Kiplinger, J. L. *J. Am. Chem. Soc.* **2007**, *129*, 11914–11915. (b) Graves, C. R.; Schelter, E. J.; Cantat, T.; Scott, B. L.; Kiplinger, J. L. *Organometallics* **2008**, *27*, 5371–5378. (c) Graves, C. R.; Scott, B. L.; Morris, D. E.; Kiplinger, J. L. *Organometallics* **2008**, *27*, 3335–3337. (d) Graves, C. R.; Vaughn, A. E.; Schelter, E. J.; Scott, B. L.; Thompson, J. D.; Morris, D. E.; Kiplinger, J. L. *Inorg. Chem.* **2008**, *47*, 11879–11891. (e) Graves, C. R.; Yang, P.; Kozimor, S. A.; Vaughn, A. E.; Clark, D. L.; Conradson, S. D.; Schelter, E. J.; Scott, B. L.; Thompson, J. D.; Hay, P. J.; Morris, D. E.; Kiplinger, J. L. *J. Am. Chem. Soc.* **2008**, *130*, 5272–5285. (f) Graves, C. R.; Scott, B. L.; Morris, D. E.; Kiplinger, J. L. *Chem. Commun.* **2009**, 776–778.

(5) (a) Arney, D. S. J.; Burns, C. J. *J. Am. Chem. Soc.* **1993**, *115*, 9840–9841. (b) Warner, B. P.; Scott, B. L.; Burns, C. J. *Angew. Chem., Int. Ed.* **1998**, *37*, 959–960. (c) Maynadie, J.; Berthet, J.-C.; Thuery, P.; Ephritikhine, M. *Chem. Commun.* **2007**, 486–488.

*To whom correspondence should be addressed. E-mail: boncella@lanl.gov.

(1) Fox, A. R.; Bart, S. C.; Meyer, K.; Cummins, C. C. *Nature* **2008**, *455*, 341–349.

(2) (a) Evans, W. J.; Davis, B. L. *Chem. Rev.* **2002**, *102*, 2119–2136. (b) Evans, W. J.; Nyce, G. W.; Johnston, M. A.; Ziller, J. W. *J. Am. Chem. Soc.* **2000**, *122*, 12019–12020. (c) Evans, W. J.; Nyce, G. W.; Ziller, J. W. *Angew. Chem., Int. Ed.* **2000**, *39*, 240–242. (d) Diaconescu, P. L.; Arnold, P. L.; Baker, T. A.; Mindiola, D. J.; Cummins, C. C. *J. Am. Chem. Soc.* **2000**, *122*, 6108–6109. (e) Evans, W. J.; Kozimor, S. A.; Ziller, J. W.; Kaltsoyannis, N. *J. Am. Chem. Soc.* **2004**, *126*, 14533–14547. (g) Evans, W. J.; Kozimor, S. A.; Ziller, J. W. *Chem. Commun.* **2005**, 4681–4683. (f) Evans, W. J.; Takase, M. K.; Ziller, J. W.; DiPasquale, A. G.; Rheingold, A. L. *Organometallics* **2009**, *28*, 236–243.

In metal-based reductions, many electron transfer processes originate from U(III)³ or U(IV)⁴ materials and produce novel uranium(IV) or uranium(V) complexes. The synthesis of uranium(VI) materials by oxidative methods can also be achieved from midvalent uranium synthons, but examples of this type are rare and typically involve the formation of new U=L multiple bonds (L = O, NR).⁵ The study of uranium(V) complexes and their ability to participate in electron transfer chemistry remains notably absent in this area of oxidation chemistry. Development of the chemistry of U(V)/U(VI) materials to accomplish catalytic redox processes with organic substrates remains an attractive and unexplored area of actinide chemistry.

One class of pentavalent uranium complexes that has displayed promise in electron transfer chemistry is the UO₂⁺ ion. Driven by their potential to promote photocatalysis and their promise as electric power storage materials,⁶ the number of well-characterized complexes of UO₂⁺ has dramatically increased in recent years and has provided insight into the importance of cation–cation interactions in structural U(V) chemistry and magnetic interactions between f¹-metal centers in polynuclear UO₂⁺ complexes.⁷ Uranyl(V) complexes also hold intrigue for their role in electron transfer chemistry because the most common decomposition pathway for UO₂⁺ complexes involves disproportionation reactions to form U(IV) and UO₂²⁺. Although these findings highlight instability associated with some of these complexes, this does suggest that pentavalent UO₂⁺ complexes hold promise for the transfer of electrons to organic substrates. This premise is further supported by recent studies highlighting the oxidation of the UO₂⁺ ion to form hexavalent UO₂²⁺ complexes with oxidizing agents such as O₂, I₂, and CH₂Cl₂.⁷ⁱ

Recently, we described the synthesis of the dimeric bis(imido) uranium(V) complex [U(N^tBu)₂(I)(^tBu₂bpy)]₂ (**1**) (^tBu₂bpy = 4,4'-di-*tert*-butyl-2,2'-bipyridyl), an isoelectronic analog of the uranyl(V) ion.⁸ The isolation of the [U(NR)₂]⁺ ion has encouraged us to explore its reactivity and draw comparisons to UO₂⁺ chemistry to further develop our understanding of pentavalent uranium complexes with metal–ligand multiple bonds. Like many examples of the UO₂⁺ ion, complex **1** features cation–cation interactions between two [U(NR)₂]⁺ ions and constitutes the first example of a nitrogenous polymetallic actinide system that contains this type of interaction. Not only does this complex exhibit antiferromagnetic coupling between uranium centers at low

temperatures, but this species can also participate as a two-electron reducing agent toward 4-methylmorpholine N-oxide to provide an oxo-bridged dinuclear bis(imido) uranium(VI) complex. This finding has sparked our interest in the discovery of other substrates that can participate in these two-electron oxidative addition reactions.

In this work, we report the synthesis of a bis(imido) uranium(V) thiolate complex [U(N^tBu)₂(SPh)(^tBu₂bpy)]₂ (**2**) by an iodide metathesis reaction and the ability of **1** and **2** to undergo oxidative addition reactions with I₂, AgX (X = Cl, Br), PhEPh (E = S, Se, Te), and chalcogen atom transfer reagents to yield bis(imido) uranium(VI) complexes. In some cases, this provides bis(imido) uranium(VI) complexes that are inaccessible by other synthetic procedures.

Experimental Section

Methods and Materials. All reactions and subsequent manipulations were performed under anaerobic and anhydrous conditions either under high vacuum conditions or in a glovebox under an atmosphere of helium or argon. Hexanes and THF were dried by passage over activated alumina, and CH₂Cl₂ was purchased anhydrous and stored over activated 4 Å molecular sieves for 24 h before use. CD₂Cl₂ and C₅D₅N were dried over activated 4 Å molecular sieves for 24 h before use. [U(N^tBu)₂(I)(^tBu₂bpy)]₂,⁸ **1**, and NaSPh · 1/4THF⁹ were synthesized by published procedures or modified published procedures. All other reagents were purchased from commercial suppliers and used as received. NMR spectra were recorded on a Bruker AVA300 spectrometer. ¹H and ¹³C{¹H} NMR spectra are referenced to external SiMe₄ using the residual protio solvent peaks as internal standards (¹H NMR experiments) or the characteristic resonances of the solvent nuclei (¹³C NMR experiments). Elemental analyses were performed at the UC Berkeley Microanalytical Facility, on a Perkin-Elmer Series II 2400 CHNS analyzer.

Synthesis of [U(N^tBu)₂(SPh)(^tBu₂bpy)]₂ (2**).** To a THF suspension of **1** (250 mg, 0.16 mmol) was added a THF solution (2 mL) of NaSPh · 1/4THF (49 mg, 0.32 mmol). The dark brown solution was stirred for 1 h and the solvent removed to dryness. Toluene (5 mL) was added to give a brown suspension which was then filtered through Celite, layered with an equal volume of hexanes, and left to stand at –30 °C for 2 days. The brown solid which precipitated was collected and then recrystallized from CH₂Cl₂/hexanes to yield large brown crystals of **2** · 2CH₂Cl₂. Under vacuum conditions, the crystalline material obtained readily loses cocrystallized CH₂Cl₂ (mass = 176 mg, yield = 72%).

¹H NMR (CD₂Cl₂): δ –25.60 (br s, 9H, –NC(CH₃)₃), –6.88 (br s, 2H, –bpyH), –4.16 (br s, 2H, –SArH), –2.75 (br s, 9H, –C(CH₃)₃), 3.04 (br s, 9H, –C(CH₃)₃), 5.50 (br s, 1H, –SArH), 6.54 (br s, 2H, –bpyH), 8.65 (br s, 2H, –bpyH), 9.22 (br s, 2H, –SArH), 41.30 (br s, 9H, –NC(CH₃)₃). Anal. Calcd. for C₆₄H₉₄N₈U₂: %C, 52.30; %H, 6.25; %N, 7.39. Found: %C, 52.37; %H, 6.31; %N, 7.43.

Synthesis of U(N^tBu)₂(I)₂(^tBu₂bpy) (3**).** To a CH₂Cl₂ (2 mL) solution of **1** (250 mg, 0.16 mmol) was added a CH₂Cl₂ (2 mL) solution of I₂ (41 mg, 0.16 mmol). A rapid color change from dark brown to red was observed and the solution stirred for 1 h. The solvent was removed in vacuo and the residue dissolved in THF to yield a bright red solution, which was filtered through Celite, layered with an equal volume of hexanes, and left to stand at –30 °C for 2 days. The red microcrystalline solid that precipitated was collected and then recrystallized from CH₂Cl₂/hexanes to yield large red crystalline material (mass = 282 mg,

(6) (a) Jørgensen, C. K.; Reisfeld, R. *Struct. Bonding (Berlin)* **1982**, *50*, 121–172. (b) Jørgensen, C. K.; Reisfeld, R. *J. Electrochem. Soc.* **1983**, *130*, 681–684. (c) Burns, C. J.; Eisen, M. S. *Organoactinide Chemistry: Synthesis and Characterization*. In *The Chemistry of the Actinide and Transactinide Elements*, 3rd ed.; Morss, L. R.; Edelstein, N. M.; Fuger, J., Eds.; Springer: Berlin, 2006; Vol. 1.

(7) (a) Natrajan, L.; Burdet, F.; Pecaut, J.; Mazzanti, M. *J. Am. Chem. Soc.* **2006**, *128*, 7152–7153. (b) Berthet, J.-C.; Siffredi, G.; Thuery, P.; Ephritikhine, M. *Chem. Commun.* **2006**, 3184–3186. (c) Burdet, F.; Pecaut, J.; Mazzanti, M. *J. Am. Chem. Soc.* **2006**, *128*, 16512–16513. (d) Hayton, T. W.; Wu, G. *Inorg. Chem.* **2008**, *47*, 7415–7423. (e) Hayton, T. W.; Wu, G. *J. Am. Chem. Soc.* **2008**, *130*, 2005–2014. (f) Nocton, G.; Horeglad, P.; Pecaut, J.; Mazzanti, M. *J. Am. Chem. Soc.* **2008**, *130*, 16633–16645. (g) Hayton, T. W.; Wu, G. *Inorg. Chem.* **2009**, *48*, 3065–3072. (h) Berthet, J.-C.; Siffredi, G.; Thuery, P.; Ephritikhine, M. *Dalton Trans.* **2009**, DOI: 10.1039/b820659g. (i) Horeglad, P.; Nocton, G.; Filinchuk, Y.; Pecaut, J.; Mazzanti, M. *Chem. Commun.* **2009**, *14*, 1843–1845.

(8) Spencer, L. P.; Schelter, E. J.; Yang, P.; Gdula, R. L.; Scott, B. L.; Thompson, J. D.; Kiplinger, J. L.; Batista, E. R.; Boncella, J. M. *Angew. Chem., Int. Ed.* **2009**, *48*, 3795.

(9) Bartucz, T. Y.; Golombek, A.; Lough, A. J.; Maltby, P. A.; Morris, R. H.; Ramachandran, R.; Schlaf, M. *Inorg. Chem.* **1998**, *37*, 1555.

yield = 96%). In the case of **3**, the NMR spectra are identical to previously published spectra.¹⁰

Synthesis of U(N^tBu)₂(X)(^tBu₂bpy) (X = Cl (4**), Br (**5**)).** The following procedure is representative of the synthesis of **4** and **5**. To a CH₂Cl₂ (2 mL) solution of **1** (250 mg, 0.16 mmol) was added a CH₂Cl₂ (2 mL) solution of AgCl (46 mg, 0.32 mmol). A rapid color change from dark brown to red is observed and the solution stirred for 1 h. The solvent was removed in vacuo and the residue dissolved in THF to yield a bright red solution, which was filtered through Celite, layered with an equal volume of hexanes, and left to stand at -30 °C for 2 days. The red microcrystalline solid that precipitated was collected and then recrystallized from CH₂Cl₂/hexanes to yield large red crystalline material (mass = 245 mg, yield = 94%).

Compound **4**. ¹H NMR (CD₂Cl₂), -30 °C: δ -0.092 (s, 18H, -NC(CH₃)₃), 1.59 (s, 9H, -C(CH₃)₃), 1.61 (s, 9H, -C(CH₃)₃), 8.11 (d, *J* = 5 Hz, 1H, -bpyH), 8.21 (d, *J* = 5 Hz, 1H, -bpyH), 8.65 (br s, 2H, -bpyH), 10.76 (d, *J* = 5 Hz, 1H, -bpyH), 10.85 (d, *J* = 5 Hz, 1H, -bpyH). ¹³C{¹H} NMR (CD₂Cl₂), -30 °C: δ 30.2 (-C(CH₃)₃), 30.8 (-C(CH₃)₃), 31.9 (-C(CH₃)₃), 57.3 (-C(CH₃)₃), 57.4 (-C(CH₃)₃), 78.9 (-C(CH₃)₃), 123.2 (-bpyC), 123.4 (-bpyC), 125.6 (-bpyC), 125.9 (-bpyC), 149.0 (-bpyC), 149.2 (-bpyC), 158.6 (-bpyC), 158.8 (-bpyC), 166.1 (-bpyC), 166.4 (-bpyC). Anal. Calcd for C₂₆H₄₂ClIN₄U: %C, 38.50; %H, 5.22; %N, 6.91. Found: %C, 38.46; %H, 5.19; %N, 6.83.

Compound **5**. ¹H NMR (CD₂Cl₂): δ 0.050 (s, 18H, -NC(CH₃)₃), 1.59 (br s, 18H, -C(CH₃)₃), 8.07 (d, *J* = 5 Hz, 1H, -bpyH), 8.11 (d, *J* = 5 Hz, 1H, -bpyH), 8.65 (br s, 2H, -bpyH), 10.75 (d, *J* = 5 Hz, 1H, -bpyH), 10.78 (d, *J* = 5 Hz, 1H, -bpyH). ¹³C{¹H} NMR (CD₂Cl₂): δ 30.0 (-C(CH₃)₃), 30.6 (-C(CH₃)₃), 31.3 (-C(CH₃)₃), 55.7 (-C(CH₃)₃), 56.1 (-C(CH₃)₃), 77.2 (-C(CH₃)₃), 122.4 (-bpyC), 122.5 (-bpyC), 124.1 (-bpyC), 124.2 (-bpyC), 148.3 (-bpyC), 148.7 (-bpyC), 157.5 (-bpyC), 158.0 (-bpyC), 164.9 (-bpyC), 165.3 (-bpyC). Anal. Calcd for C₂₆H₄₂BrIN₄U: %C, 36.50; %H, 4.88; %N, 6.59.

Synthesis of U(N^tBu)₂(EPh)(^tBu₂bpy); E = S (6**), Se (**8**), Te (**10**).** The following procedure is representative of the synthesis of **6**, **8**, and **10**. To a CH₂Cl₂ (2 mL) solution of **1** (200 mg, 0.13 mmol) was added a CH₂Cl₂ (2 mL) solution of PhSSPh (28 mg, 0.13 mmol). A gradual color change from dark brown to red was observed, and the solution was stirred for 4 h. The solvent was removed in vacuo and the residue dissolved in THF to yield a bright red solution, which was filtered through Celite, layered with an equal volume of hexanes, and left to stand at -30 °C for 2 days. The red microcrystalline solid that precipitated was collected and then recrystallized from CH₂Cl₂/hexanes to yield large red crystals (mass = 119 mg, yield = 52%). X-ray-quality crystals of **8** were obtained by slowly cooling a hot toluene solution of **8** to -40 °C. Complex **6** appears to be in equilibrium with the diiodide species U(N^tBu)₂(I)₂(^tBu₂bpy) (**3**) and U(N^tBu)₂(SPh)₂(^tBu₂bpy) (**7**). Similar findings were observed for complexes **8** (in equilibrium with **3** and U(N^tBu)₂(SePh)₂(^tBu₂bpy) (**9**)) and **10** (in equilibrium with **3** and U(N^tBu)₂(TePh)₂(^tBu₂bpy) (**11**)). Satisfactory elemental analysis was obtained for complexes **6** and **8**; however, analysis of U(N^tBu)₂(TePh)(I)(^tBu₂bpy) repeatedly contained amounts of U(N^tBu)₂(I)₂(^tBu₂bpy) (**3**) and U(N^tBu)₂(TePh)₂(^tBu₂bpy) (**11**). In the case of dichalcogenate complexes **7**, **9**, and **11**, the NMR spectra are in agreement with previously published results.¹⁰

Compound **6**. ¹H NMR (CD₂Cl₂): δ -0.092 (s, 18H, -NC(CH₃)₃), 1.57 (br s, 9H, -C(CH₃)₃), 1.60 (br s, 9H, -C(CH₃)₃), 6.88 (m, 1H, -*p*-SArH), 7.23 (m, 2H, -*m*-SArH), 8.03–8.12

(m, 2H, -*bpy*H and m, 2H, -*o*-SArH), 8.62 (br s, 2H, -*bpy*H), 10.68 (d, *J* = 5 Hz, 1H, -*bpy*H), 10.96 (d, *J* = 5 Hz, 1H, -*bpy*H). ¹³C{¹H} NMR (CD₂Cl₂): δ 29.7 (-C(CH₃)₃), 29.8 (-C(CH₃)₃), 34.8 (-C(CH₃)₃), 52.3 (-C(CH₃)₃), 52.5 (-C(CH₃)₃), 71.0 (-C(CH₃)₃), 123.0 (-bpyC), 123.2 (-bpyC), 123.5 (-ArC), 126.1 (-bpyC), 126.4 (-bpyC), 128.2 (-ArC), 129.8 (-ArC), 147.3 (-bpyC), 147.5 (-bpyC), 152.4 (-ArC), 153.7 (-bpyC), 153.9 (-bpyC), 164.0 (-bpyC), 164.1 (-bpyC). Anal. Calcd for C₃₂H₄₇IN₄SU: %C, 43.44; %H, 5.36; %N, 6.33. Found: %C, 43.38; %H, 5.20; %N, 6.40.

Compound **8**. ¹H NMR (CD₂Cl₂): δ -0.056 (s, 18H, -NC(CH₃)₃), 1.57 (br s, 9H, -C(CH₃)₃), 1.59 (br s, 9H, -C(CH₃)₃), 6.94 (m, 1H, -*p*-SeArH), 7.19 (m, 2H, -*m*-SeArH), 8.09–8.26 (m, 2H, -*bpy*H and m, 2H, -*o*-SeArH), 8.62 (br s, 2H, -*bpy*H), 10.67 (d, *J* = 5 Hz, 1H, -*bpy*H), 11.01 (d, *J* = 5 Hz, 1H, -*bpy*H). ¹³C{¹H} NMR (CD₂Cl₂): δ 32.0 (-C(CH₃)₃), 32.4 (-C(CH₃)₃), 33.2 (-C(CH₃)₃), 53.0 (-C(CH₃)₃), 53.1 (-C(CH₃)₃), 75.4 (-C(CH₃)₃), 122.7 (-bpyC), 122.8 (-bpyC), 125.8 (-ArC), 126.2 (-bpyC), 126.5 (-bpyC), 129.3 (-ArC), 133.9 (-ArC), 149.2 (-bpyC), 149.7 (-bpyC), 150.6 (-ArC), 153.0 (-bpyC), 153.2 (-bpyC), 162.8 (-bpyC), 163.1 (-bpyC). Anal. Calcd for C₃₂H₄₇IN₄SeU: %C, 41.25; %H, 5.09; %N, 6.02. Found: %C, 41.30; %H, 5.16; %N, 5.98.

Compound **10**. ¹H NMR (CD₂Cl₂): δ 0.021 (s, 18H, -NC(CH₃)₃), 1.57 (br s, 9H, -C(CH₃)₃), 1.60 (br s, 9H, -C(CH₃)₃), 6.99 (m, 1H, -*p*-TeArH), 7.17 (m, 2H, -*m*-TeArH), 8.13–8.29 (m, 2H, -*bpy*H and m, 2H, -*o*-TeArH), 8.62 (br s, 2H, -*bpy*H), 10.73 (d, *J* = 5 Hz, 1H, -*bpy*H), 11.08 (d, *J* = 5 Hz, 1H, -*bpy*H). ¹³C{¹H} NMR (CD₂Cl₂): δ 29.9 (-C(CH₃)₃), 30.4 (-C(CH₃)₃), 34.1 (-C(CH₃)₃), 51.8 (-C(CH₃)₃), 52.1 (-C(CH₃)₃), 74.0 (-C(CH₃)₃), 121.2 (-bpyC), 121.6 (-bpyC), 124.2 (-ArC), 126.0 (-bpyC), 126.4 (-bpyC), 128.2 (-ArC), 129.3 (-ArC), 146.0 (-bpyC), 146.5 (-bpyC), 153.2 (-ArC), 154.9 (-bpyC), 155.3 (-bpyC), 163.7 (-bpyC), 163.9 (-bpyC).

The syntheses of **6**, **8**, and **10** were also attempted by the addition of 1 equiv of NaEPh (E = S, Se, Te) to [U(N^tBu)₂(I)₂(^tBu₂bpy)] and by comproportionation reactions between [U(N^tBu)₂(I)₂(^tBu₂bpy)] and [U(N^tBu)₂(EPh)₂(^tBu₂bpy)]. In all examples, ¹H NMR spectroscopy indicates that concentrations of [U(N^tBu)₂(I)₂(^tBu₂bpy)], [U(N^tBu)₂(EPh)(I)(^tBu₂bpy)], and [U(N^tBu)₂(EPh)₂(^tBu₂bpy)] were nearly identical to the concentrations observed in the oxidation reactions between **1** and PhEPh.

Synthesis of U(N^tBu)₂(SPh)(SePh)(^tBu₂bpy) (12**).** The procedure for the synthesis of **12** is identical to the procedure described for the synthesis of U(N^tBu)₂(EPh)(I)(^tBu₂bpy), only starting with **2**. Satisfactory elemental analysis was not obtained due to contamination by **7** and **9** in the samples submitted. In the case of dichalcogenate complexes **7** and **9**, the NMR spectra are in agreement with previously published results.¹⁰

¹H NMR (CD₂Cl₂): δ -0.26 (s, 18H, -NC(CH₃)₃), 1.58 (br s, 18H, -C(CH₃)₃), 6.93 (m, 2H, -*p*-SArH, -*p*-SeArH), 7.20 (m, 4H, -*m*-SArH, -*m*-SeArH), 8.11 (m, 2H, -*bpy*H and m, 4H, -*o*-SArH, -*o*-SeArH), 8.65 (br s, 2H, -*bpy*H), 10.90 (d, *J* = 5 Hz, 1H, -*bpy*H), 10.95 (d, *J* = 5 Hz, 1H, -*bpy*H). ¹³C{¹H} NMR (CD₂Cl₂): δ 29.3 (-C(CH₃)₃), 30.1 (-C(CH₃)₃), 33.2 (-C(CH₃)₃), 56.1 (-C(CH₃)₃), 56.2 (-C(CH₃)₃), 73.4 (-C(CH₃)₃), 123.7 (-ArC), 123.2 (-ArC), 124.5 (-bpyC), 125.1 (-bpyC), 125.6 (-bpyC), 125.3 (-bpyC), 128.5 (-ArC), 129.9 (-ArC), 133.2 (-ArC), 133.5 (-ArC), 148.3 (-bpyC), 149.5 (-bpyC), 150.0 (-ArC), 153.0 (-bpyC), 153.7 (-bpyC), 154.1 (-ArC), 164.1 (-bpyC), 165.0 (-bpyC).

Synthesis of [U(N^tBu)₂(I)(^tBu₂bpy)]₂(μ-E) (E = O (13**), S (**14**), Se (**15**)) and [U(N^tBu)₂(I)(^tBu₂bpy)]₂(μ-η²:η²-E₄) (E = S (**16**), Se (**17**)).** The following procedure is representative of the syntheses of **13**–**17**. To a CH₂Cl₂ (2 mL) solution of **1** (300 mg, 0.19 mmol) was added a CH₂Cl₂ (2 mL) solution of 1/8S₈ (6.2 mg,

(10) Spencer, L. P.; Yang, P.; Scott, B. L.; Batista, E. R.; Boncella, J. M. *Inorg. Chem.* **2009**, *48*, 2693–2700.

0.19 mmol). The solution gradually darkens over the period of several hours, after which time the solution was filtered through Celite, layered with an equal volume of hexanes, and left to stand at $-30\text{ }^{\circ}\text{C}$ for 2 days. The red microcrystalline solid that precipitated was collected and recrystallized from $\text{CH}_2\text{Cl}_2/\text{hexanes}$ to yield large red crystals (mass = 208 mg, yield = 68%). X-ray-quality crystals of **13** and **17** were obtained in this fashion, but all attempts to obtain suitable crystals of **14–16** were unsuccessful. The spectroscopic data for **13** have been previously published.⁸

Compound **14**. ^1H NMR (CD_2Cl_2): δ 0.12 (s, 18H, $-\text{NC}(\text{CH}_3)_3$), 1.61 (s, 9H, $-\text{C}(\text{CH}_3)_3$), 1.62 (s, 9H, $-\text{C}(\text{CH}_3)_3$), 8.06 (d, $J = 5\text{ Hz}$, 1H, $-\text{bpyH}$), 8.17 (d, $J = 5\text{ Hz}$, 1H, $-\text{bpyH}$), 8.66 (br s, 2H, $-\text{bpyH}$), 11.40 (d, $J = 5\text{ Hz}$, 1H, $-\text{bpyH}$), 11.52 (d, $J = 5\text{ Hz}$, 1H, $-\text{bpyH}$). $^{13}\text{C}\{^1\text{H}\}$ NMR (CD_2Cl_2): δ 29.4 ($-\text{C}(\text{CH}_3)_3$), 31.3 ($-\text{C}(\text{CH}_3)_3$), 31.7 ($-\text{C}(\text{CH}_3)_3$), 49.4 ($-\text{C}(\text{CH}_3)_3$), 49.9 ($-\text{C}(\text{CH}_3)_3$), 77.2 ($-\text{C}(\text{CH}_3)_3$), 118.5 ($-\text{bpyC}$), 118.8 ($-\text{bpyC}$), 122.1 ($-\text{bpyC}$), 122.8 ($-\text{bpyC}$), 124.0 ($-\text{bpyC}$), 124.1 ($-\text{bpyC}$), 153.2 ($-\text{bpyC}$), 153.4 ($-\text{bpyC}$), 161.4 ($-\text{bpyC}$), 161.8 ($-\text{bpyC}$). Anal. Calcd for $\text{C}_{52}\text{H}_{84}\text{I}_2\text{N}_8\text{SeU}_2$: %C, 39.45; %H, 5.35; %N, 7.08. Found: %C, 39.51; %H, 5.40; %N, 7.14.

Compound **15**. ^1H NMR (CD_2Cl_2): δ 0.17 (s, 18H, $-\text{NC}(\text{CH}_3)_3$), 1.59 (s, 9H, $-\text{C}(\text{CH}_3)_3$), 1.61 (s, 9H, $-\text{C}(\text{CH}_3)_3$), 8.01 (d, $J = 5\text{ Hz}$, 1H, $-\text{bpyH}$), 8.14 (d, $J = 5\text{ Hz}$, 1H, $-\text{bpyH}$), 8.63 (br s, 2H, $-\text{bpyH}$), 11.44 (d, $J = 5\text{ Hz}$, 1H, $-\text{bpyH}$), 11.56 (d, $J = 5\text{ Hz}$, 1H, $-\text{bpyH}$). $^{13}\text{C}\{^1\text{H}\}$ NMR (CD_2Cl_2): δ 29.7 ($-\text{C}(\text{CH}_3)_3$), 31.0 ($-\text{C}(\text{CH}_3)_3$), 31.5 ($-\text{C}(\text{CH}_3)_3$), 49.1 ($-\text{C}(\text{CH}_3)_3$), 49.7 ($-\text{C}(\text{CH}_3)_3$), 76.8 ($-\text{C}(\text{CH}_3)_3$), 117.7 ($-\text{bpyC}$), 117.8 ($-\text{bpyC}$), 121.8 ($-\text{bpyC}$), 121.9 ($-\text{bpyC}$), 123.2 ($-\text{bpyC}$), 123.3 ($-\text{bpyC}$), 152.6 ($-\text{bpyC}$), 152.9 ($-\text{bpyC}$), 161.0 ($-\text{bpyC}$), 161.4 ($-\text{bpyC}$). Anal. Calcd for $\text{C}_{52}\text{H}_{84}\text{I}_2\text{N}_8\text{SeU}_2$: %C, 38.31; %H, 5.19; %N, 6.88. Found: %C, 38.40; %H, 5.26; %N, 7.00.

Compound **16**. ^1H NMR (CD_2Cl_2), $-45\text{ }^{\circ}\text{C}$: δ 0.13 (s, 18H, $-\text{NC}(\text{CH}_3)_3$), 1.59 (s, 9H, $-\text{C}(\text{CH}_3)_3$), 1.60 (s, 9H, $-\text{C}(\text{CH}_3)_3$), 8.04 (d, $J = 5\text{ Hz}$, 1H, $-\text{bpyH}$), 8.09 (d, $J = 5\text{ Hz}$, 1H, $-\text{bpyH}$), 8.65 (br s, 2H, $-\text{bpyH}$), 10.81 (d, $J = 5\text{ Hz}$, 1H, $-\text{bpyH}$), 11.84 (d, $J = 5\text{ Hz}$, 1H, $-\text{bpyH}$). $^{13}\text{C}\{^1\text{H}\}$ NMR (CD_2Cl_2), $-45\text{ }^{\circ}\text{C}$: δ 29.5 ($-\text{C}(\text{CH}_3)_3$), 31.4 ($-\text{C}(\text{CH}_3)_3$), 31.5 ($-\text{C}(\text{CH}_3)_3$), 49.6 ($-\text{C}(\text{CH}_3)_3$), 50.1 ($-\text{C}(\text{CH}_3)_3$), 77.0 ($-\text{C}(\text{CH}_3)_3$), 118.9 ($-\text{bpyC}$), 119.3 ($-\text{bpyC}$), 122.8 ($-\text{bpyC}$), 122.9 ($-\text{bpyC}$), 124.2 ($-\text{bpyC}$), 124.5 ($-\text{bpyC}$), 153.0 ($-\text{bpyC}$), 153.6 ($-\text{bpyC}$), 160.9 ($-\text{bpyC}$), 161.4 ($-\text{bpyC}$). Anal. Calcd for $\text{C}_{52}\text{H}_{84}\text{I}_2\text{N}_8\text{S}_4\text{U}_2$: %C, 37.19; %H, 5.04; %N, 6.67. Found: %C, 37.22; %H, 5.08; %N, 6.72.

Compound **17**. ^1H NMR (CD_2Cl_2), $-45\text{ }^{\circ}\text{C}$: δ 0.13 (s, 18H, $-\text{NC}(\text{CH}_3)_3$), 1.59 (s, 9H, $-\text{C}(\text{CH}_3)_3$), 1.61 (s, 9H, $-\text{C}(\text{CH}_3)_3$), 8.09 (d, $J = 5\text{ Hz}$, 1H, $-\text{bpyH}$), 8.12 (d, $J = 5\text{ Hz}$, 1H, $-\text{bpyH}$), 8.65 (br s, 2H, $-\text{bpyH}$), 10.81 (d, $J = 5\text{ Hz}$, 1H, $-\text{bpyH}$), 10.94 (d, $J = 5\text{ Hz}$, 1H, $-\text{bpyH}$). $^{13}\text{C}\{^1\text{H}\}$ NMR (CD_2Cl_2), $-45\text{ }^{\circ}\text{C}$: δ 29.9 ($-\text{C}(\text{CH}_3)_3$), 30.5 ($-\text{C}(\text{CH}_3)_3$), 32.0 ($-\text{C}(\text{CH}_3)_3$), 49.1 ($-\text{C}(\text{CH}_3)_3$), 49.6 ($-\text{C}(\text{CH}_3)_3$), 76.7 ($-\text{C}(\text{CH}_3)_3$), 117.9 ($-\text{bpyC}$), 118.0 ($-\text{bpyC}$), 121.9 ($-\text{bpyC}$), 122.3 ($-\text{bpyC}$), 123.7 ($-\text{bpyC}$), 123.9 ($-\text{bpyC}$), 152.7 ($-\text{bpyC}$), 153.1 ($-\text{bpyC}$), 161.3 ($-\text{bpyC}$), 161.8 ($-\text{bpyC}$). Anal. Calcd for $\text{C}_{52}\text{H}_{84}\text{I}_2\text{N}_8\text{Se}_4\text{U}_2$: %C, 33.45; %H, 4.54; %N, 6.00. Found: %C, 33.48; %H, 4.61; %N, 6.02.

X-Ray Crystallographic Details. The crystal structures of compounds **2**, **4**, **8**, **13**, and **17** were determined as follows: The crystal was mounted in a nylon cryoloop from Paratone-N oil under an argon gas flow. The data were collected on a Bruker SMART APEX II charge-coupled-device diffractometer, with a KRYO-FLEX liquid nitrogen vapor cooling device. The instrument was equipped with a graphite monochromatized Mo KR X-ray source (λ 0.71073 Å), with MonoCap X-ray source optics. A hemisphere of data was collected using ω scans, with 5 s frame exposures and 0.3° frame widths. Data collection and initial indexing and cell refinement were handled using

APEX II software.¹¹ Frame integration, including Lorentz-polarization corrections, and final cell parameter calculations were carried out using the SAINT+ software.¹² The data were corrected for absorption using the SADABS program.¹³ Decay of reflection intensity was monitored via analysis of redundant frames. The structure was solved using direct methods and difference Fourier techniques. All hydrogen atom positions were idealized and rode on the atom they were attached to. The final refinement included anisotropic temperature factors on all non-hydrogen atoms. Structure solution, refinement, graphics, and creation of publication materials were performed using SHELXTL.¹⁴

Computational Details. The B3LYP hybrid density functional was employed to optimize the equilibrium molecular structures of all of the complexes studied.¹⁵ The small-core Stuttgart RSC 1997 relativistic effective core potential (RECP) was used to model the uranium center,¹⁶ with the associate basis set [6s/6p/5d/3f]. For the ligand iodine atoms, we used the LANL2 RECP with the lanl2dz basis set. For the bridging atoms, oxygen, sulfur, and selenium, we used the all-electron basis sets 6-31G*, 6-31+G*, and 6-311+G*, respectively. For all of the nitrogen atoms, we used the 6-31+G* basis set, and for the remaining atoms in the ligands (H and C), the 6-31G* basis set was employed. The geometries of all of the molecules were optimized without symmetry constraints and were in good agreement with the experimental structure (see the Supporting Information). All of the calculations reported in this paper were carried out with the Gaussian 03 code.¹⁷

Results and Discussion

We have recently demonstrated that the iodide ligands in bis(imido) uranium(VI) complexes can undergo metathesis reactions with chalcogenate anions to yield a diverse family of bis(imido) uranium(VI) chalcogenate complexes.¹⁰ This reactivity is also observed in bis(imido) uranium(V) complexes. For example, the addition of 2 equiv of NaSPh to $[\text{U}(\text{N}^t\text{Bu})_2(\text{I})(^t\text{Bu}_2\text{bpy})_2]$ (**1**) provides the uranium(V) aryl thiolate complex $[\text{U}(\text{N}^t\text{Bu})_2(\text{SPh})(^t\text{Bu}_2\text{bpy})_2]$ (**2**) in excellent yield (eq 1). The ^1H NMR spectrum of **2** shows broad paramagnetic resonances at -25.60 and $+41.30$ ppm, which represent the *tert*-butyl imido resonances, and broad singlets at -2.75 and 3.04 ppm attributable to the *tert*-butyl groups on the bipyridyl ligand. There are also broad resonances

(11) APEX II, v. 1.08; Bruker AXS, Inc.: Madison, WI, 2004; S15.

(12) SAINT+, v. 7.06; Bruker AXS, Inc.: Madison, WI, 2003.

(13) Sheldrick, G. M. *SADABS*, v. 2.03; University of Göttingen: Göttingen, Germany, 2001.

(14) SHELXTL, v. 5.10; Bruker AXS, Inc.: Madison, WI, 1997.

(15) Becke, A. D. *J. Chem. Phys.* **1993**, *98*, 5648.

(16) Küchle, W.; Dolg, M.; Stoll, H.; Preuss, H. *J. Chem. Phys.* **1994**, *100*, 7535.

(17) Frisch, M. J.; Trucks, G. W.; Schlegel, H. B.; Scuseria, G. E.; Robb, M. A.; Cheeseman, J. R.; Montgomery, J. J. A.; Vreven, T.; Kudin, K. N.; Burant, J. C.; Millam, J. M.; Iyengar, S. S.; Tomasi, J.; Barone, V.; Mennucci, B.; Cossi, M.; Scalmani, G.; Rega, N.; Petersson, G. A.; Nakatsuji, H.; Hada, M.; Ehara, M.; Toyota, K.; Fukuda, R.; Hasegawa, J.; Ishida, M.; Nakajima, T.; Honda, Y.; Kitao, O.; Nakai, H.; Klene, M.; Li, X.; Knox, J. E.; Hratchian, H. P.; Cross, J. B.; Bakken, V.; Adamo, C.; Jaramillo, J.; Gomperts, R.; Stratmann, R. E.; Yazyev, O.; Austin, A. J.; Cammi, R.; Pomelli, C.; Ochterski, J. W.; Ayala, P. Y.; Morokuma, K.; Voth, G. A.; Salvador, P.; Dannenberg, J. J.; Zakrzewski, V. G.; Dapprich, S.; Daniels, A. D.; Strain, M. C.; Farkas, O.; Malick, D. K.; Rabuck, A. D.; Raghavachari, K.; Foresman, J. B.; Ortiz, J. V.; Cui, Q.; Baboul, A. G.; Clifford, S.; Cioslowski, J.; Stefanov, B. B.; Liu, G.; Liashenko, A.; Piskorz, P.; Komaromi, I.; Martin, R. L.; Fox, D. J.; Keith, T.; Al-Laham, M. A.; Peng, C. Y.; Nanayakkara, A.; Challacombe, M.; Gill, P. M. W.; Johnson, B.; Chen, W.; Wong, M. W.; Gonzalez, C.; Pople, J. A. *Gaussian 03*, Revision C.02; Gaussian, Inc.: Wallingford, CT, 2004.

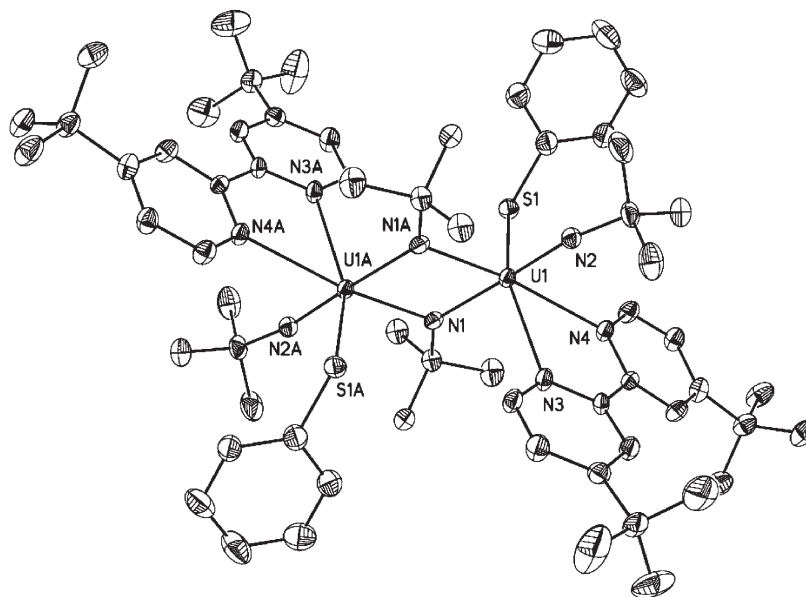
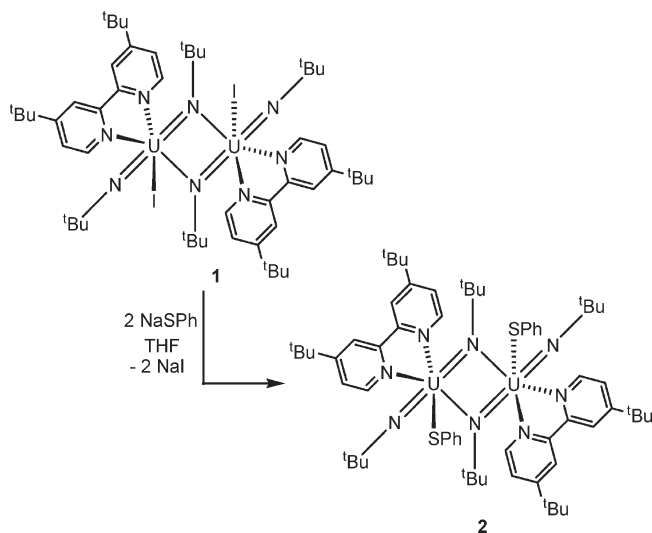


Figure 1. Solid-state molecule structure of $[U(N^tBu)_2(SPh)(^tBu_2bpy)]_2$ (**2**) with thermal ellipsoids drawn at the 50% probability level. Selected bond lengths (Å) and angles (deg): U1–N1 = 2.081(4), U1–N2 = 1.918(4), U1–N3 = 2.565(4), U1–N4 = 2.654(4), U1–N1A = 2.385(4), U1–S1 = 2.7866(18), N1–U1–N2 = 170.57(15), U1–S1–C9 = 107.48(19).

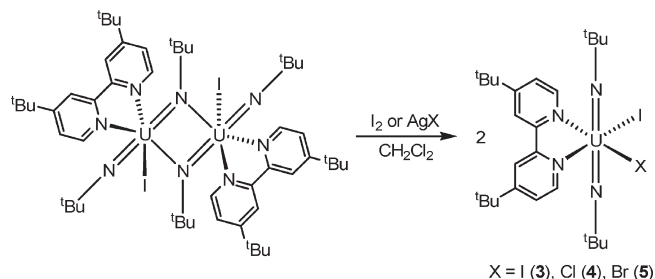
located at -4.16 , $+5.50$, and $+9.22$ ppm that can be attributed to the protons of the aryl thiolate ligand.



The solid state molecular structure of **2** is shown in Figure 1 and features similar geometrical parameters to those observed in the diiodide uranium(V) complex **1**.⁸ Complex **2** possesses a *pseudo*-octahedral geometry at each uranium center as represented by two axial bis(imido) ligands and bipyridyl, thiolate, and bridging imido equatorial ligands. A near-linear bis(imido) N=U=N bond angle (av. = 170.57(15)°) is present in **2** along with terminal U–N imido bond lengths (1.918(4) Å) that are similar to the terminal uranium(V) U–N(imido) bond distances found in $[U(N^tBu)_2(I)(^tBu_2bpy)]_2$ (av. = 1.898(5) Å).⁸ Two distinct bridging U–N(imido) bond distances are observed. The U1–N1 bond length of 2.081(4) Å suggests that some U–N multiple bond character is retained and is consistent with the U–N(imido) bond distances in other pentavalent uranium imido complexes.⁴ The other bridging U–N(imido) bond distance defined by U1–N1A (2.385(4) Å) is significantly longer and is similar to that of a reported uranium(V) amido complex.^{3d} The U–S bond length,

2.7866(18) Å, is longer than the distances observed in the uranium(V) complexes $(C_5Me_5)_2U(N-2,6-Pr_2C_6H_3)(SPh)$ (2.7230(13) Å)^{3f} and $[U(\eta^3-C_8H_8)(dddt)]_2^{2-}$ (av. U–S = 2.693(2) Å; dddt = 5,6-dihydro-1,4-dithiin-2,3-dithiolate).¹⁸

We first explored the oxidative addition chemistry of **1** with oxidizing agents such as I_2 and AgX ($X = Cl, Br$) with a goal of synthesizing bis(imido) uranium(VI) dihalide complexes. For example, the addition of 1 equiv of I_2 to $[U(N^tBu)_2(I)(^tBu_2bpy)]_2$ in CH_2Cl_2 provides the diiodo uranium(VI) species $U(N^tBu)_2(I)_2(^tBu_2bpy)$ (**3**) in near quantitative yield (eq 2). The 1H and ^{13}C NMR spectra of **3** are identical to those of previous published results.¹⁰ In the case of the mixed halide complex $U(N^tBu)_2(Cl)(I)(^tBu_2bpy)$, **4**, the room-temperature 1H NMR spectrum features broad 1H resonances that become resolved at temperatures below -30 °C, which suggests the presence of bridging chloride ligands in solution. This finding is supported by the solid-state structure of the related derivative $[U(N^tBu)_2(Cl)(\mu-Cl)(Me_2bpy)]_2$ ($Me_2bpy = 4,4'$ -dimethyl-2,2'-bipyridyl), which features bridging chloride interactions in the solid state and similar broad 1H resonances in the 1H NMR spectrum. As was observed in complex **4**, these resonances become resolved at -30 °C. Full details of this compound will be reported elsewhere.



In the solid state, these bridging chloride interactions were not observed in the molecular structure of **4**. X-ray-quality crystals of **4** were obtained from a CH_2Cl_2 /hexanes solution

(18) Arliguie, T.; Fourmigue, M.; Ephritikhine, M. *Organometallics* **2000**, *19*, 109–111.

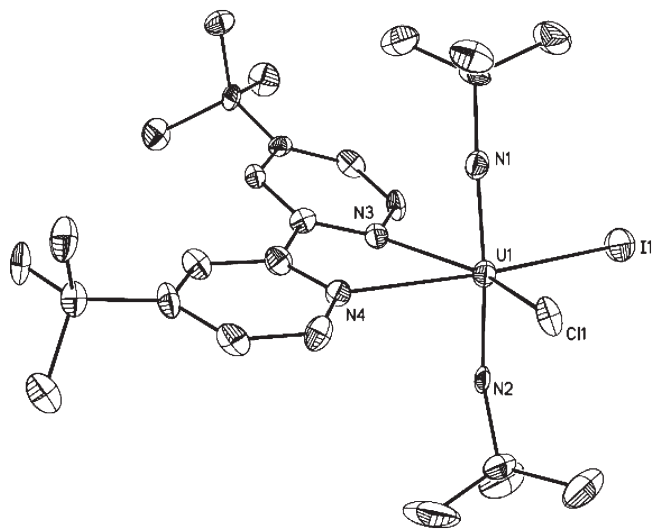
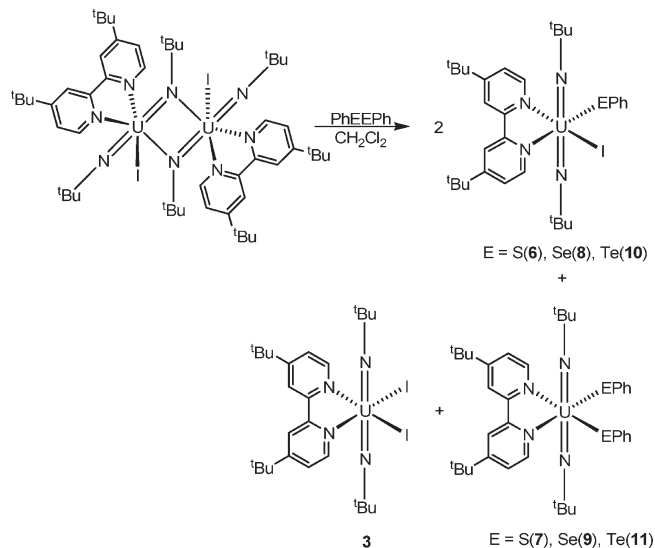


Figure 2. Solid-state molecule structure of $U(N^tBu)_2(Cl)(I)(^tBu_2bpy)$ (**4**) with thermal ellipsoids drawn at the 50% probability level. Selected bond lengths (Å) and angles (deg): U1–N1 = 1.822(6), U1–N2 = 1.822(7), U1–N3 = 2.518(7), U1–N4 = 2.524(6), U1–Cl1 = 2.7076(19), U1–I1 = 3.0419(14), N1–U1–N2 = 175.2(3).

and the solid-state molecular structure shown in Figure 2. Complex **4** is monomeric in the solid state and features a *pseudo*-octahedral environment at the uranium center with *cis*-oriented halide and *trans*-oriented bis(imido)ligands. The U–N(imido) (av. 1.822(7) Å) and U–N(bpy) bond lengths (av. 2.521(7) Å) are comparable to bond lengths found in other *trans*-disposed bis(imido) uranium(VI) complexes as is the U–I bond distance (3.0419(14) Å).^{10,19} Although U–Cl bond lengths of bis(imido) uranium(VI) complexes have yet to be reported, the U–Cl bond distance in **4** (2.7076(19) Å) is similar to the average U–Cl bond lengths found in $UO_2Cl_2 \cdot (THF)_3$ (av. 2.693(2) Å).²⁰

To further demonstrate their ability to participate in multielectron oxidative addition chemistry, complexes **1** and **2** were treated with PhEPh ($E = S, Se, Te$) to determine if E–E bond cleavage could be achieved. Indeed, the addition of PhEPh to complex **1** generates mixed iodo-chalcogenate complexes with the general formula $U(N^tBu)_2(EPh)(I)(^tBu_2bpy)$ ($E = S$ (**6**), Se (**8**), Te (**10**); eq 3). In the case of the reaction between **1** and PhSSPh to generate $U(N^tBu)_2(SPh)(I)(^tBu_2bpy)$ (**6**), the ¹H NMR spectrum features a C_s symmetric species in solution with well-defined unsymmetric bipyrindyl aryl resonances at 10.68 and 10.96 ppm. The remaining bipyrindyl aryl and *tert*-butyl resonances are overlapping with resonances attributable to two other C_{2v} symmetric complexes in solution. These complexes are present in minor amounts and are identified as the symmetrical diiodide complex $U(N^tBu)_2(I)_2(^tBu_2bpy)$ (**3**) and the dichalcogenate complex $U(N^tBu)_2(SPh)_2(^tBu_2bpy)$ (**7**) (eq 2). In addition, the mixed iodo-chalcogenate complex **6** exhibits a *tert*-butyl imido resonance at –0.092 ppm that is distinctive from the *tert*-butyl imido ligand resonances in **3** (+0.12 ppm) and **7**

(–0.29 ppm). A similar scrambling of iodide and chalcogenolate ligands is also observed in the reactions that produce $U(N^tBu)_2(SePh)(I)(^tBu_2bpy)$ (**8**) and $U(N^tBu)_2(TePh)(I)(^tBu_2bpy)$ (**10**), giving the symmetrical dichalcogenate complexes $U(N^tBu)_2(SePh)_2(^tBu_2bpy)$ (**9**) and $U(N^tBu)_2(TePh)_2(^tBu_2bpy)$ (**11**) as byproducts.



The solid-state molecular structure of **8** is shown in Figure 3 and features a uranium center in a *pseudo*-octahedral geometry with *cis*-oriented chalcogenate and iodide ligands. The U–N(imido), U–N(bpy), and U–I bond distances are comparable to other structurally characterized bis(imido)-uranium(VI) complexes.¹⁰ The U–Se bond distance of 2.8229(10) Å is also similar to the previously characterized uranium(VI) selenolate complexes $U(N^tBu)_2(SePh)_2(Me_2bpy)$ (av. 2.8224(5) Å) and shorter than the average U–Se bond lengths found in $U(N^tBu)_2(SePh)_2(OPPh_3)_2$ (2.8868(8) Å).¹⁰ Furthermore, the U–E–C_{ipso} bond angle of 106.0(6)° is also similar to average angles found in these *trans*-dichalcogenate uranium(VI) complexes ($U(N^tBu)_2(SePh)_2(OPPh_3)_2$ (106.4(2)°); $U(N^tBu)_2(SePh)_2(Me_2bpy)$ (106.69(14)°)).¹⁰

The dimeric uranium(V) thiolate complex **2** also undergoes similar oxidative addition chemistry with I_2 and PhEPh ($E = S, Se$). Following the procedures described in the oxidation of **1**, the mixed iodo-chalcogenate complex $U(N^tBu)_2(SPh)(I)(^tBu_2bpy)$ (**6**) and symmetrical chalcogenate complex $U(N^tBu)_2(SPh)_2(^tBu_2bpy)$ (**7**) are generated by the addition of I_2 and PhSSPh to $[U(N^tBu)_2(SPh)(^tBu_2bpy)]_2$ (**2**), respectively. Interestingly, the mixed dichalcogenate complex $U(N^tBu)_2(SPh)(SePh)(^tBu_2bpy)$ (**12**) can also be synthesized by the addition of 1 equiv of PhSeSePh to complex **2**. ¹H NMR spectroscopy of the product recovered from this reaction indicates the formation of $U(N^tBu)_2(SPh)(SePh)(^tBu_2bpy)$ (**12**). Minor amounts of the symmetrical dichalcogenate complexes $U(N^tBu)_2(SPh)_2(^tBu_2bpy)$ (**7**) and $U(N^tBu)_2(SePh)_2(^tBu_2bpy)$ (**9**) are also observed. The ¹H NMR spectrum of **12** features a C_s symmetric species in solution with well-defined unsymmetric bipyrindyl aryl resonances at 10.90 and 10.95 ppm. The remaining bipyrindyl aryl and *tert*-butyl resonances are overlapping with the resonances attributable to two other C_{2v} symmetric complexes in solution, $U(N^tBu)_2(SPh)_2(^tBu_2bpy)$ (**7**) and $U(N^tBu)_2(SePh)_2(^tBu_2bpy)$ (**9**). Furthermore, the *tert*-butyl imido

(19) Hayton, T. W.; Boncella, J. M.; Scott, B. L.; Palmer, P. D.; Batista, E. R.; Hay, P. J. *Science* **2005**, *310*, 1941–1943. (b) Hayton, T. W.; Boncella, J. M.; Scott, B. L.; Batista, E. R.; Hay, P. J. *J. Am. Chem. Soc.* **2006**, *128*, 10549–10559. (c) Spencer, L. P.; Yang, P.; Scott, B. L.; Batista, E. R.; Boncella, J. M. *J. Am. Chem. Soc.* **2008**, *130*, 2930–2931. (d) Spencer, L. P.; Gdula, R. L.; Hayton, T. W.; Scott, B. L.; Boncella, J. M. *Chem. Commun.* **2008**, 4986–4988.

(20) Wilkerson, M. P.; Burns, C. J.; Paine, R. T.; Scott, B. L. *Inorg. Chem.* **1999**, *38*, 4156–4158.

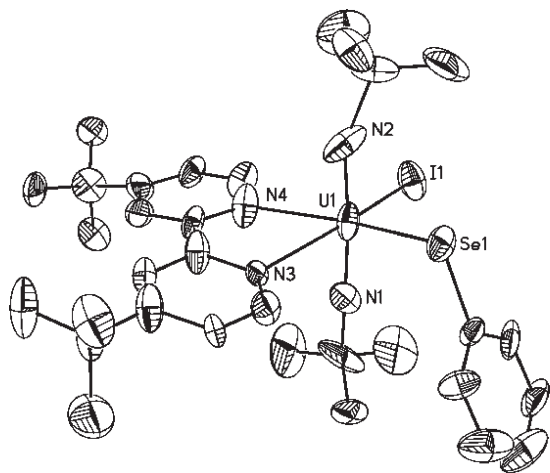
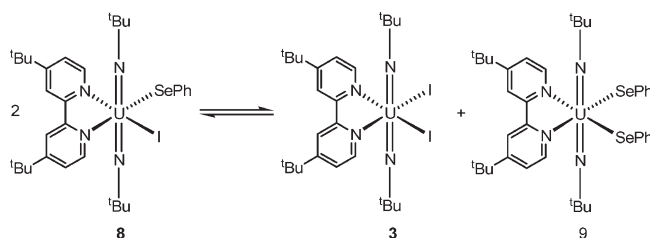


Figure 3. Solid-state molecule structure of $U(N^tBu)_2(SePh)(I)(^tBu_2bpy)$ (**8**) with thermal ellipsoids drawn at the 50% probability level. Selected bond lengths (Å) and angles (deg): $U1-N1=1.828(7)$, $U1-N2=1.819(7)$, $U1-N4=2.535(7)$, $U1-N3=2.592(18)$, $U1-Se1=2.8229(10)$, $U1-I1=3.0261(8)$, $N2-U1-N1=174.7(4)$, $C27-Se1-U1=106.0(6)$.

resonance for $U(N^tBu)_2(SPh)(SePh)(^tBu_2bpy)$ (**12**) appears at -0.26 ppm, which is significantly different than analogous resonances for $U(N^tBu)_2(SPh)_2(^tBu_2bpy)$ (**7**, -0.29 ppm) and $U(N^tBu)_2(SePh)_2(^tBu_2bpy)$ (**9**, -0.23 ppm).¹⁰

The formation of three unique uranium(VI) species in these reductive cleavage reactions implies that an equilibrium between $U(N^tBu)_2(X)(EPh)(^tBu_2bpy)$ ($X = I, E = S, Se, Te$; $X = SPh, E = Se$) and symmetrical complexes $U(N^tBu)_2(I)_2(^tBu_2bpy)$ and $U(N^tBu)_2(EPh)_2(^tBu_2bpy)$ (eq 4) is established. In the case of the iodo-selenolate complex $U(N^tBu)_2(I)(SePh)(^tBu_2bpy)$ (**8**), this equilibrium was examined in two different ways: (1) the synthesis of **8** was attempted by the addition of 1 equiv of NaSePh to $U(N^tBu)_2(I)_2(^tBu_2bpy)$ (**3**), and (2) equimolar amounts of $U(N^tBu)_2(I)_2(^tBu_2bpy)$ (**3**) and $U(N^tBu)_2(SePh)_2(^tBu_2bpy)$ (**9**) were mixed together to determine if comproportionation occurs to yield complex **8**. In both cases, 1H NMR spectroscopy of the products generated in these reactions reveals the formation of **3**, **8**, and **9** in concentrations that are nearly identical to those observed in the oxidation of **1** with PhSeSePh. This equilibrium was further investigated qualitatively by the addition of $U(N^tBu)_2(I)_2(^tBu_2bpy)$ (**3**) to a mixture of **3**, **8**, and **9** to evaluate changes to the concentration of **8**. As can be seen in Figure S1 (Supporting Information), the addition of **3** causes the concentration of **8** to increase (as indicated by the integration of the o - H_{bpy} resonances in **3**, **8**, and **9**), which further supports the presence of an equilibrium.



Given the ease with which this equilibrium is established, these findings suggest that $U-E$ ($E = S, Se, Te, I$) bonds in bis(imido) uranium(VI) complexes possess a labile nature. While this finding may reflect a weak interaction between a “hard” uranium(VI) center and “soft” halide/chalcogenate

donors, we are further investigating these and similar observations in other bis(imido) uranium(VI)–“soft” donor complexes.

As was previously communicated, complex **1** can also behave as a multielectron reductant toward 4-methylmorpholine N -oxide to yield the oxo-bridged bis(imido) uranium(VI) complex **13** (Scheme 1).⁸ This chemistry can also be extended to include the sulfur- and selenium-bridged uranium(VI) complexes **14** and **15**. For example, the addition of 1/8 equiv of S_8 to complex **1** in CH_2Cl_2 yields the chalcogenide-bridged uranium(VI) complex **14**. While all attempts to obtain X-ray-quality crystals of **14** and **15** have been unsuccessful, elemental analysis and 1H and ^{13}C NMR spectroscopy agree with the structures proposed in Scheme 1. The 1H NMR spectrum of **14** is nearly identical to the reported spectrum of **13** and features unsymmetrical bpy resonances at 8.06, 8.17, 8.66, 11.40, and 11.52 ppm and a singlet at 0.12 ppm that confirms the presence of a *tert*-butyl imido ligand. Two singlets are observed at 1.61 and 1.62 ppm that are assigned to the methyl groups on the bpy ligand which further supports the presence of an unsymmetric bpy ligand.

The solid state molecular structure of **13** was determined by X-ray crystallography; the thermal ellipsoid plot is shown in Figure 4. Complex **13** features both uranium centers in a *pseudo*-octahedral geometry and $U-N$ (imido) and $U-I$ bond distances that are similar to those in other reported *trans*-bis(imido) uranium(VI) complexes.^{10,19} The average $U-O$ bond distances (2.104(9) Å) are significantly shorter than observed in other uranium(VI) phenolate complexes but are significantly longer than $U-O$ (oxo) bond lengths found in $[UO_2]^{2+}$ complexes.²¹ For example, the uranyl(VI) complex $[UO_2(O-2,6-Ph_2C_6H_3)(THF)_2]$ is representative of many complexes of the $[UO_2]^{2+}$ ion and features a $U-O$ (oxo) bond distance of 1.759(14).^{21b} Additionally, a near-linear $U-O-U$ bond angle ($173.3(6)^\circ$) is observed that suggests some measure of $U-O$ multiple bond character present in the solid state in **13**. Similar findings have also been observed in other uranium complexes that possess single-atom chalcogenide donors that bridge between uranium metal centers.^{3c,f,g} It is believed that, in many of these examples, a π interaction occurs between the chalcogenide donor and uranium center, which explains the short $U-E$ bond distances and near linear $U-E-U$ bond angle.

Further insight into the orbital interactions between the uranium and chalcogen atoms found in **13–15** was obtained from theoretical calculations with the model complexes $[(U(N^tBu)_2(I)(bpy))_2(\mu-E)]$ ($E = O$ (**13'**), S (**14'**), Se (**15'**)). The computational tools were tested comparing the solid-state molecular structure of **13** with the model complex of the oxo-bridged dimer $[(U(N^tBu)_2(I)(bpy))_2(\mu-O)]$, **13'**. Good structural agreement is observed in the calculated $U-O$ distance (within 1.5%) as well as the $U-O-U$ angle (173.77° (theoretical) versus 173.3° (experimental)). The rest of the common structural parameters, namely, $U-bpy$, are also in good agreement and reported in the Supporting Information. In the $U-O-U$ interaction in **13'**, there are two orbital interactions between uranium 6d and 5f orbitals and oxygen 2p orbitals that possess π symmetry (Figure 5). Presumably, these π interactions account for both the short

(21) (a) Barnhart, D. M.; Burns, C. J.; Sauer, N. N.; Watkin, J. G. *Inorg. Chem.* **1995**, *34*, 4079–4084. (b) Wilkerson, M. P.; Burns, C. J.; Morris, D. E.; Paine, R. T.; Scott, B. L. *Inorg. Chem.* **2002**, *41*, 3110–3120.

Scheme 1

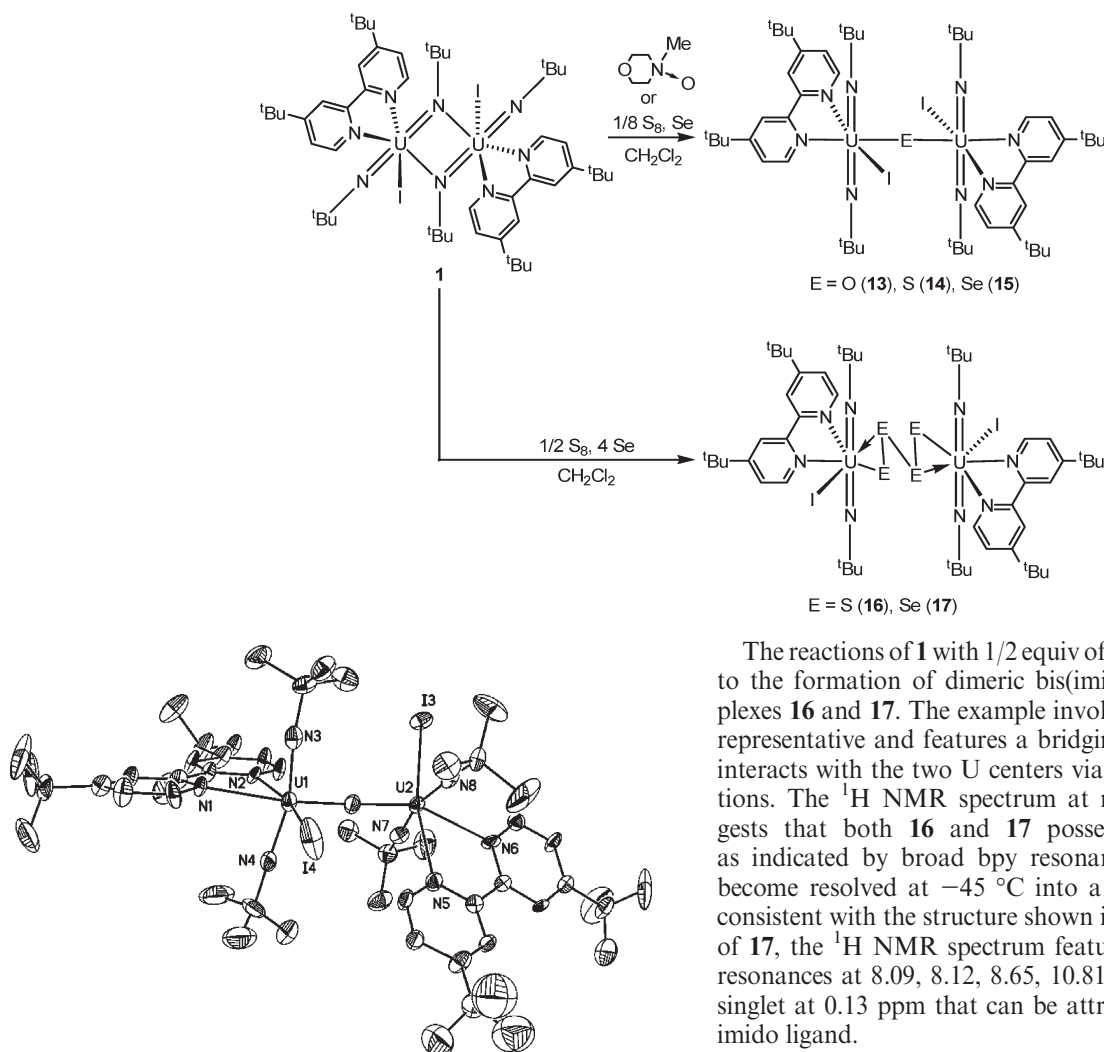


Figure 4. Solid-state molecular structure of $[(U(N^tBu)_2(I)(^tBu_2bpy))_2(\mu-O)]$ (**13**) with ellipsoids shown at the 50% probability level. Selected bond lengths (Å) and angles (deg): U1–O1 = 2.102(10), U1–N1 = 2.533(11), U1–N2 = 2.515(12), U1–N3 = 1.840(15), U1–N4 = 1.856(16), U1–I4 = 3.0657(14), U2–O1 = 2.106(10), N3–U1–N4 = 165.6(6), U1–O1–U2 = 173.3(6).

U–O bond distances and the near-linear U–O–U bond angle and support the presence of U–O multiple bond character in the solid state in **13**.

The geometry-optimized models **13'**–**15'** also show interesting features in the U–E–U bond angle. In the case of the oxygen and sulfur derivatives **13'** and **14'**, the U–E–U angles are near linear (E = O, 173.77°; E = S, 179.87°); however the selenium-bridged dimer is bent with an angle of 159.30°. Although solid-state molecular information has yet to be obtained for the sulfur- and selenium-bridged compounds to support the theoretical findings, these results are consistent with the U–S–U angle found in the dinuclear uranium–sulfide bridged complex $[(ArO)_3U_2(\mu-S)]$ (U–S–U = 180.0(1)°; Ar = 2,6-di-*tert*-butylphenoxide) but significantly different than the U–S–U angle found in $[(MeC_5H_4)_3U_2(\mu-S)]$ (164.9(4)°). While the reasons for these discrepancies are not clear, we are currently examining the importance of s-hybridization of the E atoms in U–E–U bonding interaction as the size of the E atom becomes larger.

The reactions of **1** with 1/2 equiv of S_8 or 4 equiv of Se leads to the formation of dimeric bis(imido) uranium(VI) complexes **16** and **17**. The example involving Se (complex **17**) is representative and features a bridging $[Se_4]^{2-}$ ligand which interacts with the two U centers via two η^2-Se_2-U interactions. The 1H NMR spectrum at room temperature suggests that both **16** and **17** possess a fluxional nature, as indicated by broad bpy resonances. These resonances become resolved at -45 °C into a set of signals that are consistent with the structure shown in Scheme 1. In the case of **17**, the 1H NMR spectrum features unsymmetrical bpy resonances at 8.09, 8.12, 8.65, 10.81, and 10.94 ppm and a singlet at 0.13 ppm that can be attributed to the *tert*-butyl imido ligand.

The solid-state molecular structure of **17** is shown in Figure 6 and was determined from a single-crystal X-ray diffraction experiment performed on crystals grown from a CH_2Cl_2 /hexanes solution. Both uranium centers are formally seven-coordinate and feature U–N(imido) and U–I bond distances that are similar to other reported *trans*-bis(imido) uranium(VI) complexes.^{10,19} The interactions between the uranium center and η^2-Se_2 ligand are not symmetrical, as shown by the differences in U1–Se1 and U1–Se2 bond distances. The distance observed in U1–Se1 (2.9175(8)) is longer than the U–Se bond distances found in $U(N^tBu)_2(SePh)(I)(^tBu_2bpy)$ (**8**; 2.8229(10) Å) and suggests an anionic interaction between this Se atom and uranium. In contrast, the U1–Se2 bond length is significantly longer than U1–Se1 (~0.1 Å), which suggests a dative interaction between U and Se atoms. The Se1–Se2 bond distance (2.2756(10) Å) in the η^2-Se_2 portion of the ligand is significantly shorter than the Se2–Se2A (2.4152(14) Å) bond length that connects the ligating Se atoms in the $(Se_4)^{2-}$ ligand. Although the reason for this discrepancy in bond distances is not clear, the latter value is reminiscent of Se–Se bond lengths found in the tetraselenide complexes $[MoO(Se_4)]^{2-}$ (av. 2.378(2) Å) and $[W(Se_4)_2]^{2-}$ (av. 2.401(2) Å).²²

(22) Wardle, R. W. M.; Mahler, C. H.; Chau, C.-N.; Ibers, J. A. *Inorg. Chem.* **1988**, *27*, 2190–2795.

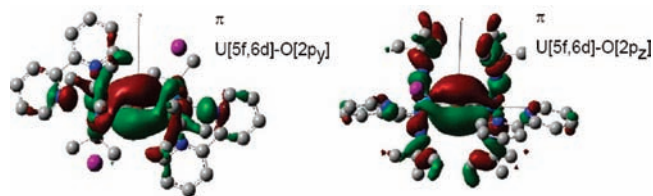


Figure 5. Graphical representation of the uranium–oxygen π -bonding molecular orbitals involved in the U–O bonds of $[(U(N^tBu)_2(I)(bpy))_2(\mu-O)]$ (**13'**).

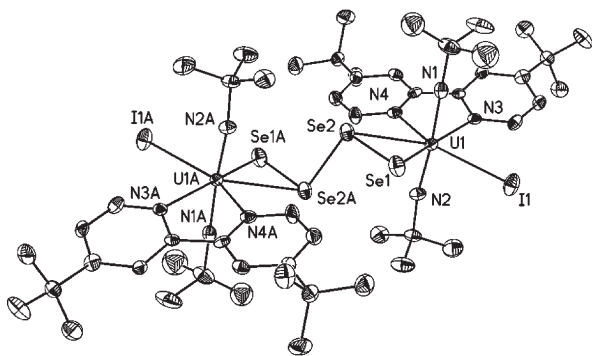


Figure 6. Solid-state molecule structure of $[U(N^tBu)_2(I)(^tBu_2bpy)]_2(\mu-\eta^2:\eta^2-Se_4)$ (**17**) with thermal ellipsoids drawn at the 50% probability level. Selected bond lengths (Å) and angles (deg): U1–Se1 = 2.9175(8), U1–Se2 = 3.0013(8), U1–N1 = 1.830(5), U1–N2 = 1.837(5), U1–N3 = 2.569(5), U1–N4 = 2.558(5), U1–I1 = 3.0604(7), Se1–Se2 = 2.2756(10), Se2–Se2A = 2.4152(14), N1–U1–N2 = 172.4(2), U1–Se1–Se2 = 69.35(3), U1–Se2–Se1 = 65.46(3), Se1–U1–Se2 = 45.19(2).

In conclusion, we report that the dimeric bis(imido) uranium(V) iodide complex **1** can undergo metathesis reactions with NaSPh to generate the uranium(V) aryl thiolate complex $[U(N^tBu)_2(SPh)(^tBu_2bpy)]_2$ (**2**). Both the uranium(V) complexes **1** and **2** can undergo oxidative addition reactions with I_2 , AgX (X = Cl, Br), PhEPh (E = S, Se, Te), and chalcogen atom transfer reagents to yield bis(imido) uranium(VI) complexes that, in some cases, cannot be

synthesized using more conventional procedures. This ability to behave as reducing agents (to undergo oxidative addition reactions) appears to be driven to a significant extent by the formation of the *trans*-U(VI) bis(imido) framework. The observed reactions are similar to the synthesis of the bis(imido) uranium(VI) diiodide starting materials in which the U(VI) complexes are generated by an oxidant (I_2) that is not strong enough to generate U(VI) in the absence of the formation of the U=N multiple bonds. Related reactivity has been observed in the oxidation of Ce(III) triamido amine complexes by I_2 to give Ce(IV) products, which is likely driven by the formation of strong Ce(IV) amide bonds because the (aqueous) redox potentials of the reagents suggest that the reaction should not proceed.²³

While electron transfer reactivity toward these organic substrates has yet to be applied in a catalytic manner, the facile nature with which E–E bonds can be broken with pentavalent bis(imido) uranium molecules suggests that similar oxidative addition reactions may have utility in U(V)–U(VI)-mediated catalysis. Current efforts are focused on the reduction of these U(VI) materials to determine if catalytic conversion can be achieved. We are also investigating the two-electron reduction of other chemical bonds to give new U(VI) complexes.

Acknowledgment. P.Y. and L.P.S. thank the Seaborg Institute for their postdoctoral fellowships. E.R.B. was partially supported by the Division of Chemical Sciences, Office of Basic Energy Sciences, U.S. Department of Energy under the Heavy Element Chemistry program at LANL. We thank the Center for Integrated Nanotechnology at LANL for computing support. LANL is operated by Los Alamos National Security, LLC, for the National Nuclear Security Administration of the U.S. D.O.E. under contract DEAC52-06NA25396.

Supporting Information Available: Complete X-ray crystallographic details (as a CIF file) of **2**, **4**, **8**, **13**, and **17**. Geometries of the calculated structures of **13'**–**15'**. Equilibrium studies of **3**, **8**, and **9**. This material is available free of charge via the Internet at <http://pubs.acs.org>.

(23) Morton, C.; Alcock, N. W.; Lees, M. R.; Munslow, I. J.; Sanders, C. J.; Scott, P. J. *Am. Chem. Soc.* **1999**, *121*, 11255–11256.